Hyperspectral images as function-valued mappings, their self-similarity and a class of fractal transforms

E.R. Vrscay[1] D. Otero[1] Davide La Torre[2]

Department of Applied Mathematics, Faculty of Mathematics,
University of Waterloo, Waterloo, ON, Canada

Department of Economics, Business and Statistics,
University of Milan, Milan Italy

ervrscay@uwaterloo.ca, dotero@uwaterloo.ca, davide.latorre@unimi.it

ICIAR 2013, Povoa de Varzim, Portugal, June 26-28, 2013

Outline

This study represents ongoing work on the development of **multifunction representations** of images, in particular,

- **Measure-valued image functions:**
  - D. La Torre, E.R.V., M. Ebrahimi, M.F. Barnsley, Measure-valued images, associated fractal transforms and the affine self-similarity of images, SIAM J Imaging Sciences **2** (2), 470-507 (2009)
  - D. La Torre and E.R.V., Random measure-valued image functions, fractal transforms and self-simlilarity, Applied Mathematics Letters **24**, 1405-1410 (2011)
- **Function-valued image functions:**
  - O. Michailovich, D. La Torre and E.R.V., Function-valued mappings, total variation and compressed sensing for diffusion MRI, ICIAR 2012.
  - I.C. Salgado Patarroyo, S. Dolui, O.V. Michailovich and E.R.V., Reconstruction of HARDI data using a split Bregman optimization approach, ICIAR 2013.

Our work is involved with generalizations of the usual mathematical representation of a (greyscale/colour) image, i.e.,

$$u : X \longrightarrow R_g,$$

where

- X: **base** or **pixel space**, the support of the image, $X \subset \mathbb{R}^n$, $n = 1, 2, 3$,
- $R_g \subset \mathbb{R}$ (or $\mathbb{R}^3$): the **greyscale** (or **colour**) **range**.

Representations of image functions

Greyscale-valued image function

At each pixel $x \in X$, $u(x)$ is a **real value** (or a vector of real values, i.e., "RGB")

Function-valued image function

At each pixel $x \in X$, $u(x)$ is a **real-valued function**, i.e., $u(x;t)$

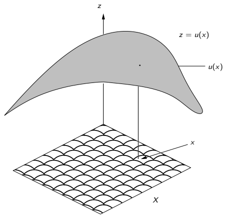

(a) Greyscale-valued image function

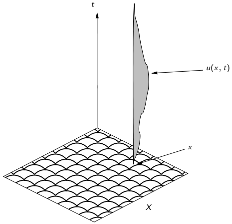

(b) Function-valued image function

Example: In multispectral/hyperspectral imaging, u represents the **spectral density function**. The values $u(x, t_k)$, $t_1 < t_2 < \cdots < t_M$ represent intensities of reflected radiation from point x on ground, as captured by satellite reading, at a discrete set of wavelengths, t_k.

Hyperspectral imaging

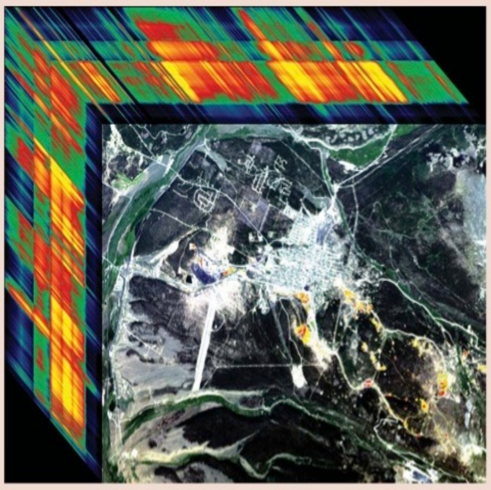

In practical situations, multispectral/hyperspectral images may be represented by **vector-valued functions**,

$$u : X \to \mathbb{R}^M,$$

i.e.,

$$u(x) = (u_1(x), u_2(x), \cdots, u_M(x)),$$

where

$$u_k : X \to \mathbb{R}, \quad 1 \leq k \leq M$$

are the usual real-valued **image functions**. (Of course, RGB images are special, low-dimensional, cases.)

That being said, it is instructive to start with the continuous, multifunction approach, from which definitions over vector-valued image functions naturally follow.

Outline

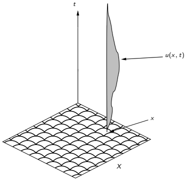

(a)

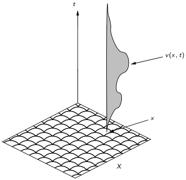

(b)

Linear space: For $u, v : X \to L^2(R_g)$, define

$$(c_1 u + c_2 v)(x, t) = c_1 u(x, t) + c_2 v(x, t), \quad \text{etc. (linear space)}$$

Normed linear space Y: For $u : X \to L^2(R_g)$, norm of $u(x)$ is given by

$$\|u(x)\|^2_{L^2(R_g)} = \int_{R_g} u(x, t)^2 \, dt.$$

Integrate over all $x \in X$ to define norm of u:

$$\|u\|^2_Y = \int_X \|u(x)\|^2_{L^2(R_g)} \, dx.$$

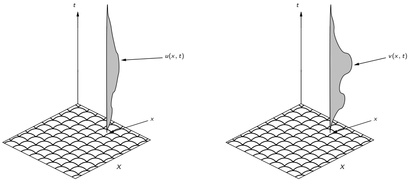

(a) (b)

Complete metric space (Y, d_Y):

1. At each $x \in X$, compute L^2 distance between functions $u(x)$ and $v(x)$:

$$\|u(x) - v(x)\|^2_{L^2(R_g)} = \int_{R_g} [u(x,t) - v(x,t)]^2 \, dt$$

2. Integrate over all $x \in X$:

$$[\, d_Y(u,v)\,]^2 = \int_X \|u(x) - v(x)\|^2_{L^2(R_g)} \, dx.$$

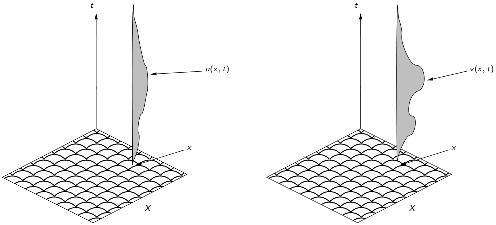

(a) (b)

Hilbert space:
Since $u(x), v(x) \in L^2(R_g)$, we may compute their inner product $\langle u(x), v(x) \rangle_{L^2(R_g)}$. Integrate over all $x \in X$ to define inner product between function-valued image mappings,

$$\langle u, v \rangle_Y = \int_X \langle u(x), v(x) \rangle_{L^2(R_g)} \, dx, \quad u, v \in Y.$$

Complete metric space (Y, d_Y) of function-valued image mappings

$$Y = \{u : X \to L^2(R_g) \mid \|u\|_Y < \infty\}$$

where

$$\|u\|_Y^2 = \int_X \|u(x)\|_{L^2(R_g)}^2 \, dx$$

In our applications,

$$R_g = [a, b] \subset R_+ = [0, \infty).$$

Outline

Self-similarity of greyscale images

S.K. Alexander, E.R.V. and S. Tsurumi, A simple, general model for the affine self-similarity of images, ICIAR 2008

It was shown that images generally possess a considerable degree of **affine self-similarity**, i.e.,

Subblocks of an image are well approximated by a number of other subblocks – with the possible help of affine greyscale transformations

Self-similarity of images has been implicitly used in a number of **nonlocal image processing schemes**, including

- Nonlocal-means denoising (A. Buades, B. Coll and J.M. Morel 2005, 2010).
- Method of "self-examples," and "examples" in general (e.g., BM3D method of K. Dabov *et al.*, IEEE Trans. Image Proc. 2007).
- Fractal image coding (N. Lu, *Fractal Imaging*, Academic Press 1997).
- Yes, vector quantization! (Fractal image coding is, in fact, "self-vector quantization".)

A simple model of affine image self-similarity

For simplicity, consider the discrete case: X is an $n_1 \times n_2$ pixel array. Then:

1. Let $\mathcal{R}$ be a set of $n \times n$-pixel **range** subblocks R_i, $1 \leq i \leq N_R$, such that $\cup_i R_i = X$. (For convenience, assume that they are nonoverlapping.)
2. Let $\mathcal{D}$ denote a set of $m \times m$-pixel **domain** subblocks D_j, $1 \leq j \leq N_D$, where $m \geq n$ and $\cup_i D_i = X$.
3. Let $w_{ij} : D_j \to R_i$ denote affine geometric transformation (along with decimation, if necessary). There are 8 possible mappings of squares to squares - here we consider only one (no rotation/flipping).

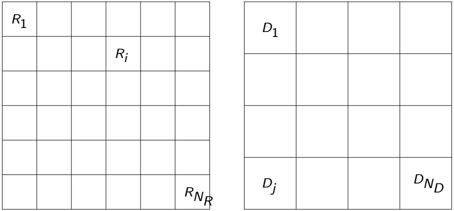

In ICIAR08 study, 8×8-pixel range blocks R_j and 8×8- or 16×16-pixel domain blocks were used.

How well are subimages $u(R_i)$ approximated by subimages $u(D_j)$?

$$u(R_i) \approx \phi_i u(w_{ij}^{-1}(R_i)), \qquad 1 \leq i \leq N_R,$$

where $\phi_i : \mathbf{R} \to \mathbf{R}$ is a **greyscale transformation**.

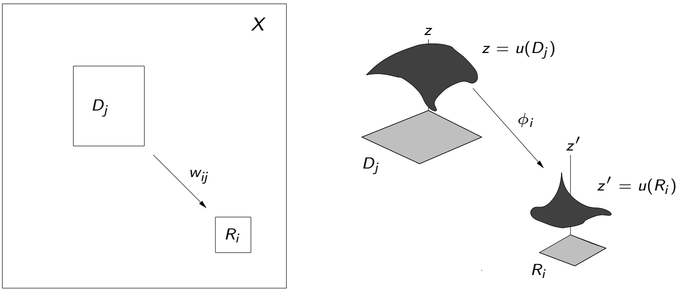

Left: Range block R_i and associated domain block D_j. **Right:** Greyscale mapping ϕ_i from $u(D_j)$ to $u(R_i)$.

Consider **affine greyscale maps**, i.e.,

$$\phi(t) = \alpha t + \beta$$

Simple in form, yet sufficiently flexible

Then examine the distribution of L^2 (RMS) approximation errors Δ_{ij}, $1 \leq i \leq N_R$, $1 \leq j \leq N_D$:

$$\Delta_{ij} = \| u(R_i) - \phi(u(w_{ij}^{-1}(R_i))) \|_2$$

Note that all images are assumed to be **normalized**, i.e., $0 \leq u_{pq} \leq 1$, so that

$$0 \leq \Delta_{ij} \leq 1$$

Four particular cases of self-similarity considered:

1. **Case 1 (Purely translational):** The w_{ij} are translations and $\alpha_i = 1$, $\beta_i = 0$, i.e.,

$$u(R_i) \approx u(D_j)$$

   Employed in **nonlocal means denoising**

2. **Case 2 (Translational + greyscale shift):** The w_{ij} are translations and $\alpha_i = 1$, optimize β:

$$u(R_i) \approx u(D_j) + [\overline{u(R_i)} - \overline{u(D_j)}]$$

3. **Case 3 (Affine, same scale):** The w_{ij} are translations but we optimize α and β:

$$u(R_i) \approx \alpha_i u(D_j) + \beta_i$$

4. **Case 4 (Affine, cross-scale):** The w_{ij} are affine spatial **contractions** (which involve decimations in pixel space).

$$u(R_i) \approx \alpha_i u(w_{ij}^{-1}(R_i)) + \beta_i$$

   Employed in **fractal image coding**

Same-scale self-similarity – Cases 1, 2 and 3

Recall:

- **Case 1**: Purely translational
- **Case 2**: Translational + greyscale shift β
- **Case 3**: Translational + affine greyscale transformation $\alpha t + \beta$.

We expect that

$$0 \le \Delta_{ij}^{(Case\ 3)} \le \Delta_{ij}^{(Case\ 2)} \le \Delta_{ij}^{(Case\ 1)}$$

"World's most self-similar image"

The "flat" image,

$$u(x, y) = C \qquad \text{(constant)}$$

$\Delta^{(Case\ q)}$-error distributions have single peaks at $\Delta = 0$, for $q = 1, 2, 3$ and 4.

Next on the list:

"Ramped" images,

$$u(x, y) = C + Ax + By$$

$\Delta^{(Case\ q)}$-error distributions have single peaks at $\Delta = 0$, for $q = 2, 3$ and 4.

And now on to more realistic images ...

Case 1 (Purely translational)

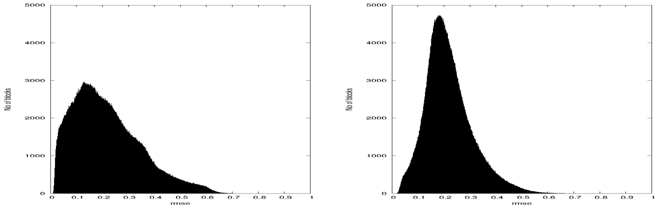

(a) Lena (b) Mandrill

Case 1 (same-scale) self-similarity error distributions $\Delta_{ij}^{(Case\ 1)} = \|u(R_j) - u(R_i)\|_2, \quad i \neq j$, for normalized 512×512-pixel *Lena* and *Mandrill* images. In all cases, 8×8-pixel blocks $R_i = D_i$ were used.

Same-scale self-similarity – Cases 1, 2 and 3

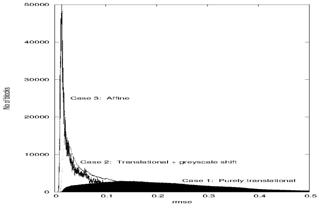

(a) Lena

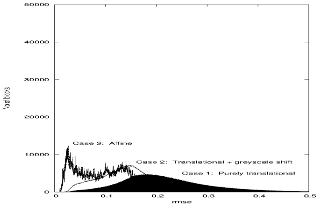

(b) Mandrill

Same-scale (Cases 1,2 and 3) RMS self-similarity error distributions for normalized *Lena* and *Mandrill* images. Again, 8×8-pixel blocks $R_i = D_i$ were used. Case 1 distributions are shaded.

Outline

Self-similarity of hyperspectral images

Assume that digital hyperspectral image is supported on an $N_1 \times N_2$ pixel array, as before, but now M channels per pixel.

At a pixel location $(i_1, i_2) \in X$, the hyperspectral image function is a non-negative M-vector with components

$$u_k(i_1, i_2), \quad 1 \leq k \leq M\,.$$

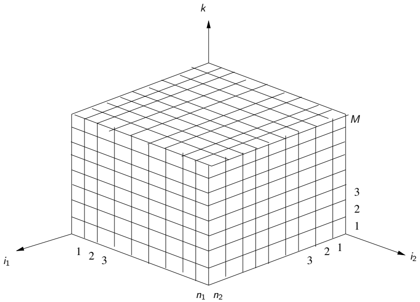

Also as before:

1. Let $\mathcal{R}$ be a set of $n \times n$-pixel **range** subblocks R_i, $1 \le i \le N_R$, such that $\cup_i R_i = X$. (For convenience, assume that they are nonoverlapping.)
2. Let $\mathcal{D}$ denote a set of $m \times m$-pixel **domain** subblocks D_j, $1 \le j \le N_D$, where $m \ge n$ and $\cup_i D_i = X$.
3. Let $w_{ij} : D_j \to R_i$ denote affine geometric transformation (along with decimation, if necessary).

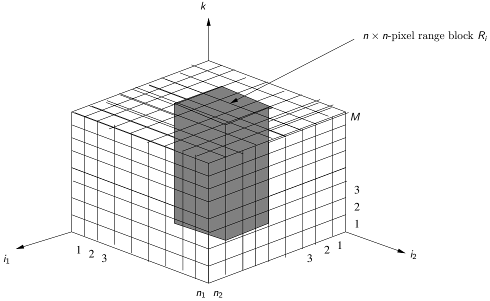

Let $u(R_i)$ denote portion of hyperspectral image function supported on subblock $R_i \in X$. Here, $u(R_i)$ will be an $n \times n \times M$ cube of nonnegative real numbers.

The L^2 (RMS) distance, Δ_{ij}, between two hyperspectral image subblocks $u(R_i)$ and $u(R_j)$ will be given by

$$\Delta_{ij} = \frac{1}{n\sqrt{M}} \left[\sum_{i_1=I_1}^{I_1+n-1} \sum_{i_2=I_2}^{I_2+n-1} \sum_{k=1}^{M} [u_k(i_1, i_2,) - u_k(i_1 + J_1, i_2 + J_2)]^2 \right]^{1/2}$$

This may also be viewed as the error associated with the (Case 1) approximation,

$$u(R_i) \approx u(R_j) \qquad \text{(Case 1)}$$

Case 2 approximations with spectral shifts

- Simplest case - the same shift, $\beta \in \mathbb{R}$, for all channels

$$u(R_i) \approx u(R_j) + \beta, \qquad \text{(Case 2(a))}$$

This does not improve the Case 1 approximation significantly.

- Separate shift, β_k, for each channel

$$u(R_i) \approx u(R_j) + \underline{\beta}, \quad \text{(Case 2(b))}$$

Componentwise,

$$u_k(i_1, i_2) \approx u_k(j_1, j_2) + \beta_k, \quad 1 \leq k \leq M$$

Case 3 approximation with affine scaling + spectral shift

$$u(R_i) \approx \alpha u(R_j) + \underline{\beta} \qquad \text{(Case 3)}$$

Note that we are using only **one** scaling coefficient α for all channels.

Note: If we used separate scaling coefficients for each channel k, i.e.,

$$u_k(R_i) \approx \alpha_k u(R_j) + \beta_k \,, \quad 1 \leq k \leq M,$$

then we are essentally treating a hyperspectral image as M separate greyscale images (which defeats the purpose of hyperspectal image analysis).

Approximation errors:

$$0 \leq \Delta_{ij}^{(Case\ 3)} \leq \Delta_{ij}^{(Case\ 2(b))} \leq \Delta_{ij}^{(Case\ 2(a))} \leq \Delta_{ij}^{(Case\ 1)}$$

Results of some computations

33-channel hyperspectral image, “Scene 2,” downloaded from webpage of D.H. Foster, University of Manchester

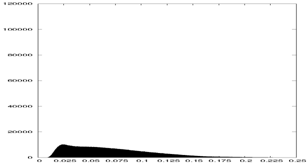

(a) Case 1

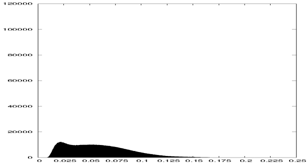

(b) Case 2(a)

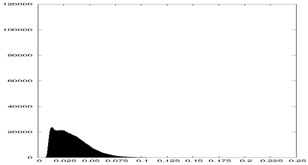

(c) Case 2(b)

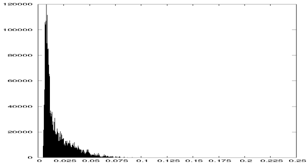

(d) Case 3)

Per-pixel error distributions $\Delta_{ij}^{(Case\ q)}$ for 33-channel HS fern image. In all cases, 8×8-pixel blocks R_i and D_j were used.

224-channel AVIRIS (Airborne Visible/Infrared Imaging Spectrometer) hyperspectral image, "Yellowstone calibrated scene 0," a 224-channel image, available from JPL.

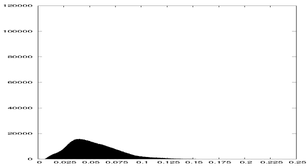

(a) Case 1

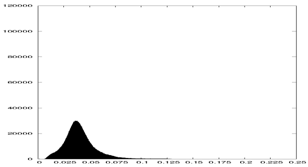

(b) Case 2(a)

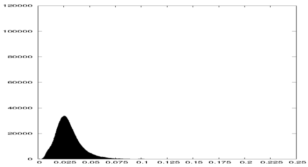

(c) Case 2(b)

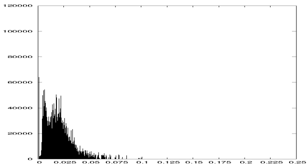

(d) Case 3

Per-pixel error distributions $\Delta_{ij}^{(Case\ m)}$ for the 224-channel AVIRIS image. In all cases, 8×8-pixel blocks R_i and D_j were used.

Single-pixel self-similarity of spectral functions

Because of the additional degree of freedom along the spectral axis, we may consider $n \times n$-pixel blocks as $n \to 1$, in particular, $n = 1$

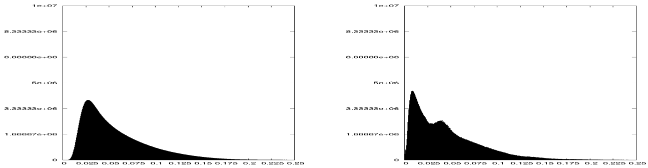

(a) Hyperspherical fern (b) Yellowstone AVIRIS

Case 1 error distributions $\Delta_{ij}^{(Case\ 1)}$ for spectral functions supported on **single-pixel** blocks R_i.

However, L^2 distance (RMSE) is not necessarily a good indicator of signal/image fidelity or correlation.

Correlation of single-pixel spectral functions

A number of alternative **quality indices** exist, e.g., "structural similarity." Here, however, we examine simple correlation $C(\mathbf{x}, \mathbf{y})$ between spectral functions $\mathbf{x}, \mathbf{y} \in \mathbb{R}^M$.

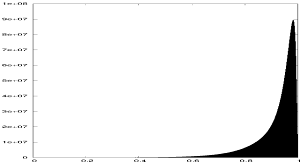

(a) Hyperspherical fern

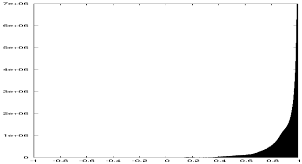

(b) Yellowstone AVIRIS

Pairwise correlations between **single-pixel** spectral functions.

The dramatic correlation demonstrated in these plots strongly suggests that single-pixel spectral functions are quite suitable for nonlocal methods of image processing.

Outline

In fractal image coding of greyscale images:

1. Affine greyscale transformations are employed, i.e.: $\phi(t) = \alpha t + \beta$.
2. Domain blocks D_j are **larger** than range blocks R_j.

As before, consider the discrete case: X is an $n_1 \times n_2$ pixel array. Then:

1. Let $\mathcal{R}$ be a set of $n \times n$-pixel **range** subblocks R_i, $1 \leq i \leq N_R$, such that $\cup_i R_i = X$. (For convenience, assume that they are nonoverlapping.)
2. Let $\mathcal{D}$ denote a set of $2n \times 2n$-pixel **domain** subblocks D_j, $1 \leq j \leq N_D$, where $m \geq n$ and $\cup_i D_i = X$.
3. Let $w_{ij} : D_j \to R_i$ denote affine geometric **contraction mapping** - in pixel domain this is accomplished by some kind of decimation/downsampling.

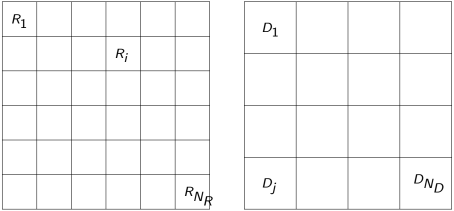

Fractal transform of greyscale image

For $1 \leq i \leq N_R$, approximate $u(R_i)$ with greyscale modified and spatially contracted (decimated) copy of $u(D_{j(i)})$:

$$\begin{aligned} u(R_i) &\approx \alpha_i u(D_{j(i)})' + \beta_i && \text{(Case 4)} \\ &= \alpha_i u(w_{ij}^{-1}(R_i)) + \beta_i \\ &=: (Tu)(R_i), \qquad 1 \leq i \leq N_R. \end{aligned}$$

T is **fractal transform operator**. (Prime denotes spatial contraction/pixel decimation.)

Fractal transform of hyperspectral image

For $1 \leq i \leq N_R$, approximate the "data cube" $u(R_i)$ with greyscale modified and spatially contracted (decimated) copy of "data cube" $u(D_{j(i)})$:

$$\begin{aligned} u(R_i) &\approx \alpha_i u(D_{j(i)})' + \underline{\beta_i} && \text{(Case 4)} \\ &= \alpha_i u(w_{ij}^{-1}(R_i)) + \underline{\beta_i} \\ &=: (Tu)(R_i), \quad 1 \leq i \leq N_R. \end{aligned}$$

T is **fractal transform operator**. (Prime denotes spatial contraction/pixel decimation.)

Note: As in Case 3 approximations of hyperspectral images, we employ **one** scaling coefficient α and a vector of shift coefficients $\underline{\beta_i}$

Contractivity of hyperspectral fractal transform operator

Under appropriate conditions on α_i, the hyperspectral fractal transform operator T is **contractive** on the metric space (Y, d_Y) of hyperspectral images.

From Banach's Fixed Point Theorem, there exists a unique $\bar{u} \in Y$ such that

$$\bar{u} = T\bar{u}.$$

Furthermore,

For any "seed" image $u_0 \in Y$, if we define the iteration procedure,

$$u_{n+1} = Tu_n,$$

then

$$d_Y(u_n, \bar{u}) \to 0 \quad \text{as} \quad n \to \infty.$$

Inverse problem for hyperspectral fractal transforms on (Y, d_Y)

Given a target element (hyperspectral image) $u \in Y$, find a contractive fractal transform $T : Y \to Y$ such that its fixed point $\bar{u}$ approximates u to a desired accuracy, i.e.,

$$d_Y(\bar{u}, u) < \epsilon.$$

Such a fractal transform T will defined by

1. The range block-domain block assignments $(i, j(i)), \quad 1 \leq i \leq N_R$,
2. The scaling coefficients a_i and $\underline{\beta_i}, \quad 1 \leq i \leq N_R$.

- The hyperspectral image u has been approximated by the fixed point $\bar{u}$ of the contractive fractal transform operator T.
- The fixed point $\bar{u}$ may be generated by iteration of T.
- **Result:** The hyperspectral image u has been **fractally coded**.

Practical fractal image coding

Most, if not all, fractal image coding methods rely on a simple consequence of Banach's Fixed Point Theorem, known as the **Collage Theorem**.

Given a contraction mapping $T : Y \to Y$ with contraction factor $c_T \in [0, 1)$ and fixed point $\bar{u}$, then for any $u \in Y$,

$$\|u - \bar{u}\| \leq \frac{1}{1 - c_T} \|u - Tu\|$$

In order to approximate the target u with a fixed point $\bar{u}$, we look for a transform T that maps the target u as close as possible to itself, i.e., we minimize the **collage distance** $\|u - Tu\|$.

This is accomplished by finding, for each range block $u(R_i)$, the domain block $u(D_{j(i)})$ that **best approximates** $u(R_i)$, i.e., minimizes the approximation error Δ_{ij}.

Example: Fractal coding of 224-channel AVIRIS "Yellowstone" image

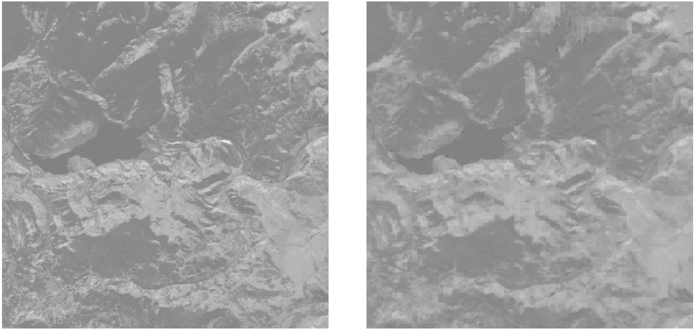

Channel 120. Left: Original. Right: Fractal-based approximation.
8×8-pixel range blocks and 16×16-domain blocks.

Example: Fractal coding of 224-channel AVIRIS "Yellowstone" image

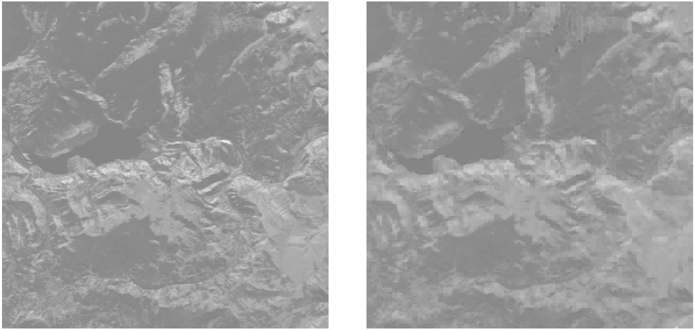

Channel 220. Left: Original. Right: Fractal-based approximation.
8×8-pixel range blocks and 16×16-domain blocks.